Electromagnetics

Waveguide Tubes Coated With Inhomogeneous Lossy Materials for Superior Shielding Above and Below Cutoff Frequency

Mohammad Almalkawi[1], Charles Bunting[2], Vijay Devabhaktuni[1], and Abdel-Razik Sebak[3]

[1] Department of Electrical Engineering and Computer Science, University of Toledo, Toledo, OH 43606, USA
[2] Department of Electrical and Computer Engineering, Oklahoma State University, Stillwater, OK 74078, USA
[3] Department of Electrical and Computer Engineering, Concordia University, Montreal, QC H3G 1M8, Canada

Received 23 May 2012, revised 12 June 2012, accepted 16 June 2012, published 24 July 2012.

Abstract—A new approach for enhanced electromagnetic interference shielding of metallic waveguide (WG) tubes coated with inhomogeneous lossy materials is proposed based on numerical simulation. Shielding enhancement is achieved by using stepped variations of complex permittivity and complex permeability coating materials along the WG transverse direction. Such variation in the coating layer provides multiple wave reflections below and above the WG cutoff frequency. The underlying principle is applied to a rectangular WG operating in the dominant TE_{10} mode. Simulation examples of rectangular WGs coated with uniform and stepped lossy materials are demonstrated. The proposed approach shows remarkably better performance when compared with WGs coated with uniform lossy materials.

Index Terms—Electromagnetics, lossy coatings, electromagnetic interference shielding, rectangular waveguide, reflection losses.

I. INTRODUCTION

Electronic systems such as wireless devices, radar systems, and television stations act as potential sources of electromagnetic interference (EMI). To mitigate external intentional and unintentional EMI sources from penetrating a device or to prevent internal RF emissions from escaping a device, metallic enclosures of electronic circuits is one of the fundamental ways to address EMI issues [Paul 2006]. EMI shielding is of interest to both military and commercial applications; the only differences are the larger shielding frequency range (10 kHz–40 GHz) and higher shielding levels (i.e., greater than 80 dB) required for military use in comparison with commercial applications (300–1000 MHz and greater than 30 dB) [Lee 1999]. Typically, for high levels of attenuation, the shield must have no penetrations (e.g., seams, slots, holes, and cables). However, this may not be an option for many applications where air ventilation is required for thermal reasons [Intel 2001]. In addition, one may have an internal RF or optical source that must penetrate the enclosure or cables interconnecting devices. In such cases, we are forced to use different shielding techniques where openings in the shield are inevitable. Waveguide (WG) tubes with metallic walls operating below the cutoff frequency f_c have been utilized as EMI shields while providing airflow into the enclosure. A WG with uniform cross section acts as a reciprocal high-pass filter where the energy below f_c is exponentially attenuated and the energy above f_c is transferred along the guide length. The cutoff frequency of a WG is determined by its cross-sectional dimensions. The larger the WG dimension, the lower the f_c, and hence, the tradeoff between shielded frequency range and the airflow capacity. Typically, a WG cross-sectional size should be selected such that its f_c remains above the highest interference frequency. One way to allow high volume of air into an enclosure is to weld WGs together in a honeycomb fashion. However, research conducted by Intel [2001] established that increasing the number of WGs in a panel decreases the shielding level for frequencies below f_c. The literature holds few publications investigating different techniques to attenuate the traveling energy above f_c [Jiao 2012, Luo 2006, Bereuter 1982]. Most recently, the idea of shielding frequencies above f_c by coating the inner walls of a WG tube with lossy materials was investigated by Jiao [2012]. His work considered the use of a circular WG that is uniformly coated with either a lossy conductive, a lossy dielectric, or a lossy magnetic material. His results show that the magnetic coating material exhibits high attenuation levels above f_c in comparison with the lossy conductive and lossy dielectric materials. The attenuation level can also be enhanced by increasing the magnetic loss angle and by increasing the thickness of the lossy coating layer. However, using lossy magnetic coating suffers from low attenuation levels for frequencies below f_c. Below f_c, the attenuation is determined by the mode attenuation, and above, by the power loss mechanism in the lossy coating layer. Hence, there is no control on the attenuation, in the low-frequency range, below f_c where the majority of EMI sources fall. To this end, the intent of this work is to demonstrate that the use of stepped lossy material to coat the inner walls of a WG tube can lead to an enhanced attenuation performance for frequencies below and above f_c. The organization of this letter is as follows. Section II discusses the analysis of a rectangular WG coated with uniform and inhomogeneous/stepped lossy materials. Section III presents the simulation results of the proposed approach with different number of coating segments along the WG length, while conclusions are given in Section IV.

II. ANALYSIS

For a minimal air flow resistance, a WG with uniform cross section is selected. WGs support an infinite number of modes,

Corresponding author: M. J. Almalkawi (malmalk@utoledo.edu).
Digital Object Identifier: 10.1109/LMAG.2012.2205374

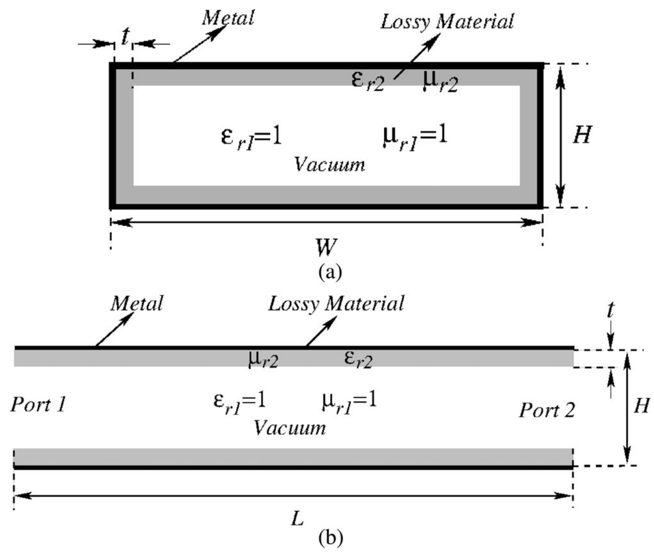

Fig. 1. Geometry of a rectangular WG coated with a uniform lossy material (lossy magnetic or lossy dielectric). (a) Aperture cross-sectional view (b) Side cross-sectional view.

each of which has their own cutoff frequency. The cutoff frequency of a rectangular WG operating in the dominant (TE_{10}) mode can be computed from [Paul 2006]

$$f_{c10} = \frac{c/\sqrt{\varepsilon_r \mu_r}}{2W}. \tag{1}$$

In (1), c is the speed of light in free space, ε_r is the relative permittivity, μ_r is the relative permeability of the material filling the WG cavity, and W is the WG width. The characteristic impedance Z_o and propagation constant γ_g of a WG is a function of frequency. For a TE_{10} mode rectangular WG, the propagation constant is given by

$$\gamma_g(\omega) = \sqrt{\omega^2 \mu\varepsilon - \left(\frac{\pi}{W}\right)^2} \tag{2}$$

where ω is the angular operating frequency; and ε and μ are the permittivity and the permeability of the WG cavity, respectively. Therefore, for a given frequency and WG mode, γ_g has a prescribed value. The wave impedance of a TE_{10} rectangular WG can be calculated from [Pozar 2012]

$$Z_o(\omega) = \frac{\omega\mu}{\gamma_g(\omega)}. \tag{3}$$

Fig. 1 shows a uniform metallic rectangular WG with its inner side coated by a uniform lossy material. It will be shown in Section III that using uniform lossy coating material has a negative attenuation impact on frequencies below f_c. Therefore, the proposed coating approach using inhomogeneous/stepped lossy material variations along the WG length, as depicted in Fig. 2, will lead to an improved EMI shielding performance. Fig. 2 shows a side cross section of a rectangular WG coated with equal length, stepped segments of lossy dielectric and magnetic materials. Such step variation will enhance the shielding performance below and above f_c by virtue of the wave impedance differences at each segment interface where wave reflections occur [Pozar 2012]. The reflection coefficient at the interface of

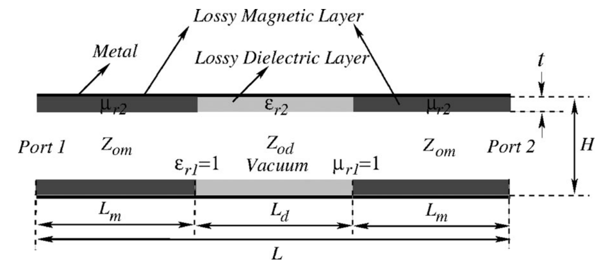

Fig. 2. Side cross-sectional view of the proposed WG coated with three segments of lossy materials. The stepped variations consist of the following order: lossy magnetic–dielectric–magnetic along the WG length L.

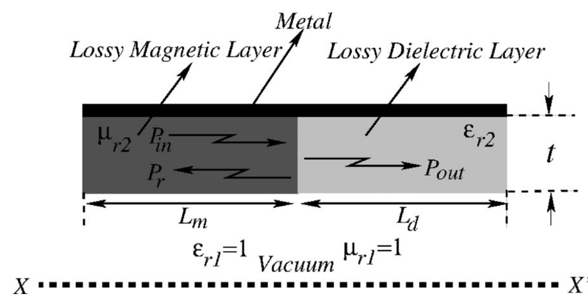

Fig. 3. Portion of a WG side cross section coated with inhomogeneous lossy layer that is comprised of a lossy magnetic and a lossy dielectric material. X–X' is the plane of symmetry.

any two segments can be calculated by

$$|\Gamma| = \left|\frac{Z_{0d} - Z_{0m}}{Z_{0d} + Z_{0m}}\right| \tag{4}$$

where Γ is the reflection coefficient, and Z_{0d} and Z_{0m} are the wave impedance of the WG coated with a lossy dielectric and a lossy magnetic material, respectively.

The intensity of the reflected waves is related to the difference of the characteristic impedances of the incident medium.

Fig. 3 depicts the reflected wave P_r and the transmitted wave P_{out} from a dielectric/magnetic interface due to the normal incidence of a TE wave (P_{in}).

The field attenuation of a WG of length L is proportional to $e^{-\gamma_g L}$ [Choubani 2006]. In a lossless WG, γ_g is a real number for frequencies below f_c. This leads to an exponentially decaying field amplitude along the guide and weak energy propagates through the guide due to evanescent modes. Moreover, γ_g is imaginary for frequencies above f_c and a varying sinusoidal field is propagating along the WG.

We found that in a lossy media, γ_g is a complex number for both above and below f_c, where the magnitude of the real part is dominant for frequencies below f_c and the magnitude of the imaginary part is dominant for frequencies above f_c; thus, a high-pass filter characteristic is maintained. In addition to the power loss mechanism of the propagating energy along the WG length, multiple wave reflections in our proposed approach will add to the attenuation levels below and above f_c. The following equation describes the relation between the input/output powers of a two segments WG tube depicted in Fig. 3

$$P_{\text{out}} = (P_{\text{in}} e^{-\gamma_{g1} L_m} e^{-\gamma_{g2} L_d} (1 - |\Gamma|^2)). \tag{5}$$

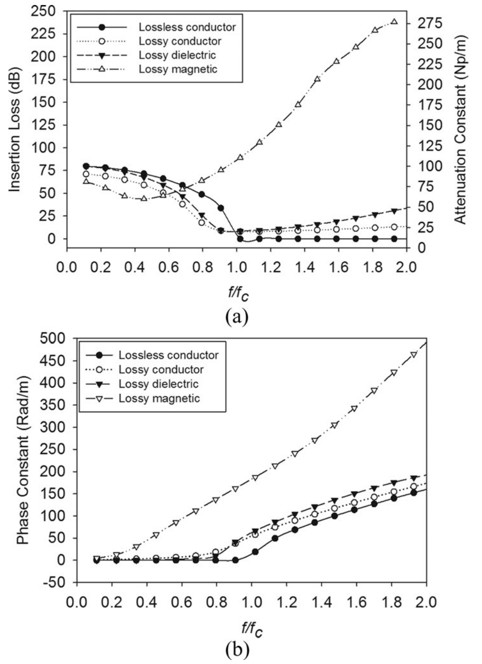

Fig. 4. (a) Insertion loss versus normalized frequency for a uniform lossless conductor, a lossy conductor, a lossy dielectric, and a lossy magnetic coating layer. (b) Phase constant behavior versus normalized frequency.

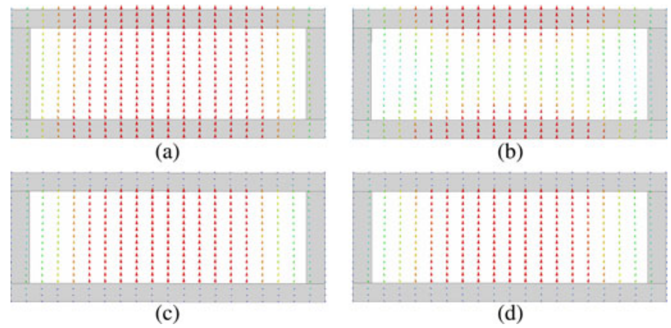

Fig. 5. Electric field distribution of the TE_{10} mode at a frequency below f_c (at 3 GHz) and above f_c (at 6 GHz) for a rectangular WG coated with (a) and (b) uniform magnetic and (c) and (d) uniform dielectric material.

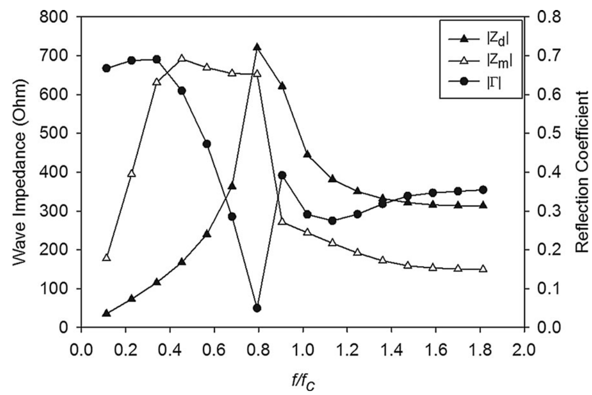

Fig. 6. Magnitude of the wave impedance for a WG coated with a uniform lossy magnetic (Z_m), a uniform lossy dielectric (Z_d), and the reflection coefficient magnitude (Γ) versus normalized frequency.

In (5), P_{in} and P_{out} are the transmitted and received powers at the WG ports, respectively; γ_{g1} and γ_{g2} are the complex propagation constants of the lossy magnetic and lossy dielectric WG segments, respectively; and L_m and L_d are the lossy magnetic and lossy dielectric segment lengths, respectively. The insertion loss (IL) or attenuation along the WG can be expressed by the forward scattering transmission coefficient (S_{21}) of a two-port network as described in the following equation:

$$\text{IL} = -20\log_{10}|S_{21}| = -10\log_{10}\frac{P_{\text{out}}}{P_{\text{in}}} \tag{6}$$

which takes into account the attenuation due to the internal wave reflections. This is in contrast to the analytical approach based on the attenuation constant presented by Jiao [2012] which is applicable only for uniformly coated WGs.

III. SIMULATION RESULTS AND DISCUSSION

In this section, rectangular WGs with uniform and stepped coating are demonstrated. In our simulation, a WG with a width W of 34 mm, a height H of 14 mm, a length L of 100 mm, and a coating thickness t of 2 mm was selected and was excited by its dominant TE_{10} mode. From (1), the WG with lossless metallic walls has an f_c of 4.41 GHz.

Full-wave electromagnetic simulations were carried out using HFSS [ANSYS 2011] on the WG tube with uniform and stepped coating. Different lossy coating materials were studied and we assumed a conductivity of $\sigma = 5$ S/m for the lossy conductive material, a permittivity of $\varepsilon_r = 15\angle 45^{\text{o}}$ for the lossy dielectric, and a permeability of $\mu_r = 15\angle 45^{\text{o}}$ for the lossy magnetic material. A lossy conductive material can be established using resistive carbon colloid and graphite, a lossy dielectric can be formed using lossy ceramics such as MgO–SiC, while a lossy magnetic material can be made by an appropriate composition of carbonyl iron/rubber powder or NiCuZn ferrite [Feng 2006, Naito 1971, Kim 1991, Dimri 2006]. Using the aforementioned design parameters, Fig. 4(a) shows that at frequencies below f_c, both lossless metals and lossy dielectric coatings exhibit high insertion loss when compared with the lossy metal and lossy magnetic coating, whereas the magnetic coating possesses dramatically high insertion loss above f_c. Fig. 4(b) depicts the dependence of the phase constant behavior on the normalized frequency. Both dielectric and magnetic coating reduces the cutoff frequency of the mode from f_c to about $0.9f_c$ and $0.5f_c$, respectively, which confirms the recently published results by Jiao [2012]. It is worth mentioning that using WG coated with lossy materials can provide an excellent attenuation performance for a broad frequency range up to $2f_c$.

Corrosion is a major drawback of metallic materials which greatly degrades effectiveness of shields. Therefore, in our approach, we will utilize only lossy magnetic and lossy dielectric as coating materials.

With magnetic coating and operation above f_c, the mode becomes a surface mode [Lee 1986] where a large field concentration within the thin coating layer is established. This explains the high attenuation levels above f_c. Fig. 5 shows the

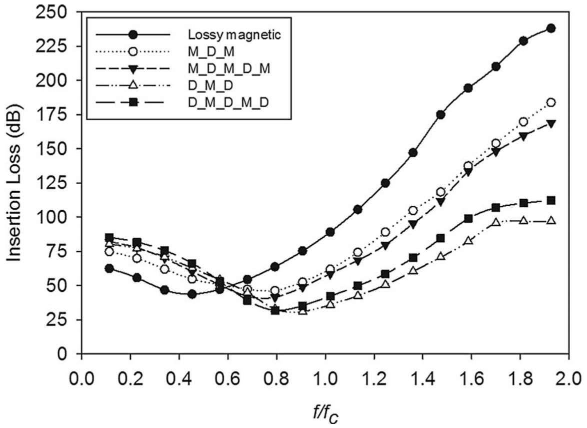

Fig. 7. Insertion loss versus normalized frequency of a uniform coating lossy magnetic layer: three and five segments of the proposed stepped coating with different coating percentage of lossy magnetic and dielectric along the WG length.

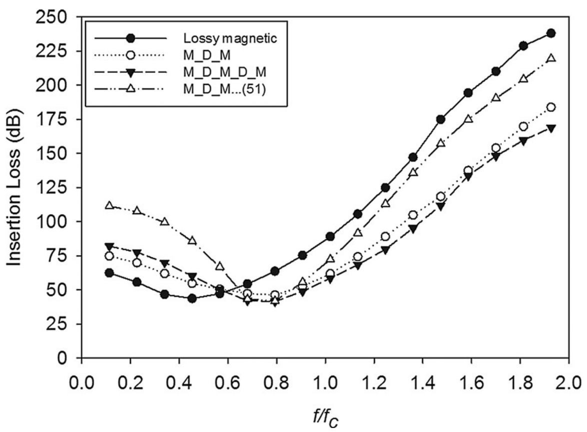

Fig. 8. Insertion loss versus normalized frequency of a uniform coating lossy magnetic layer: three, five, and 51 segments of the proposed stepped coating.

location of wave concentration for lossy dielectric and magnetic layers above and below f_c. The red color indicates strong electric field intensity, while the blue color indicates weak electric field intensity.

Fig. 6 shows the magnitude of the reflection coefficient and wave impedances of the WG uniformly coated with lossy dielectric Z_d and another coated with lossy magnetic Z_m material versus the normalized frequency. Hence, high reflections occur below and above f_c. As anticipated from (3), both materials exhibit high impedance values around f_c since γ_g possess essentially minimum values.

Fig. 7 shows the results of the proposed approach with three and five segments of coating material where M denotes magnetic coating and D denotes dielectric coating. As depicted, when the magnetic coating percentage along the WG length is greater than the dielectric coating, more attenuation is achieved above f_c with less attenuation below f_c and vice versa.

From Fig. 8, by increasing the number of coating segments up to 51 segments, the effect of multiple wave reflections positively impact the attenuation performance above and below f_c. The maximum attenuation level achieved with 51 segments at the low-frequency side was around 110 dB at 0.1f_c, and at the high-frequency side was around 220 dB at 1.9f_c.

IV. CONCLUSION

A new approach for enhancing the EMI shielding of WG tubes below and above f_c has been introduced. The method is flexible, not restricted for certain WG types or modes. The feasibility of the technique was demonstrated for a rectangular WG tube coated with stepped spatial variation along the propagation axis using lossy dielectric and lossy magnetic materials. Compared to a WG uniformly coated with a lossy magnetic material operating below and above f_c, the stepped variation provides multiple wave reflections to the incident waves in addition to the power loss effect that is inherent to a given lossy materials.

ACKNOWLEDGMENT

This work was supported by the National Science Foundation, Engineering Design and Innovation, under Grant 1000744.

REFERENCES

ANSYS High Frequency Structure Simulator (HFSS), Ansys, Inc., Canonsburg, PA, 2011.

Bereuter W A, Chang D C (1982), "Shielding effectiveness of metallic honeycombs," *IEEE Trans. Electromagn. Compat.*, vol. 24, no. 1, pp. 58–61, doi: 10.1109/TEMC.1982.304013.

Choubani F, David J, Mastorakis N E (2006), "Experiment on the shielding by hollow conducting tubes," *IEEE Trans. Electromagn. Compat.*, vol. 48, no. 2, pp. 342–347, doi: 10.1109/TEMC.2006.873872.

Dimri M C, Kashyap S C, Dube D C, Mohanta S K (2006), "Complex permittivity and permeability of Co-substituted NiCuZn ferrite at rf and microwave frequencies," *J. Electroceram.*, vol. 16, no. 4, pp. 331–335, doi: 10.1007/s10832-006-9874-4.

Feng Y B, Qiu T, Shen C Y, Li X Y (2006), "Electromagnetic and absorption properties of carbonyl iron/rubber radar absorbing materials," *IEEE Trans. Magn.*, vol. 42, no. 3, pp. 363–368, doi: 10.1109/TMAG.2005.862763.

Intel Corporation (2001). *EMI Waveguide Apertures* [Online]. Available: http://www.formfactors.org/developer%5Cspecs%5Cwg_overview_098.pdf

Jiao C (2012), "Shielding effectiveness improvement of metallic waveguide tube by using wall losses," *IEEE Trans. Electromagn. Compat.*, vol. 54, no. 3, pp. 696–699, doi: 10.1109/TEMC.2012.2187663.

Kim S S, Jo S B, Gueon K I, Kim J M, Churn K S (1991), "Complex permeability and permittivity and microwave absorption of ferrite-rubber composite in X-band frequencies," *IEEE Trans. Magn.*, vol. 27, no. 6, pp. 5462–5464, doi: 10.1109/20.278872.

Lee C S, Lee S W, Chuang S L (1986), "Normal modes in an overmoded circular waveguide coated with lossy material," *IEEE Trans. Microw. Theory Tech.*, vol. MTT-34, no. 7, pp. 773–785, doi: 10.1109/TMTT.1986.1133440.

Lee C Y, Song H G, Jang K S, Oh E J, Epstein A J, Joo J (1999), "Electromagnetic interference shielding efficiency of polyaniline mixtures and multilayer films," *Synthetic Metals*, vol. 102, pp. 1346–1349, doi: 10.1016/S0379-6779(98)00234-3.

Luo J R, Jiao C Q (2006), "Effect of lossy layer thickness of metal cylindrical waveguide wall on the propagation constant of electromagnetic modes," *Appl. Phys. Lett.*, vol. 88, no. 6, 061115, doi: 10.1063/1.2172735.

Naito Y, Suetake K (1971), "Application of ferrite to electromagnetic wave absorber and its characteristics," *IEEE Trans. Microw. Theory Tech.*, vol. MTT-19, no. 1, pp. 65–72, doi: 10.1109/TMTT.1971.1127446.

Paul C R (2006), *Introduction to Electromagnetic Compatibility*, 2nd ed. Hoboken, NJ: Wiley.

Pozar D M (2012), *Microwave Engineering*, 4th ed. Hoboken, NJ: Wiley.